



PSEUDO-DYNAMIC TESTING OF A 3D FULL-SCALE HIGH DUCTILE STEEL-CONCRETE COMPOSITE MR FRAME STRUCTURE AT ELSA

Oreste S. BURSI¹, Stefano CAMELLI², Giovanni FABBROCINO³, Artur V. PINTO⁴,
Walter SALVATORE⁵, Fabio TAUCER⁶, Robert TREMBLAY⁷ and Riccardo ZANDONINI⁸

SUMMARY

Composite moment resisting (MR) frame structures consisting of steel-concrete beams and reinforced concrete partially encased columns can provide efficient and economical alternatives to traditional steel or reinforced concrete constructions. In addition to economies achieved by effective use of different materials, this research shows the feasibility of composite MR frames with partially encased columns and partial strength beam-to-column joints to provide strength and ductility exceeding that in conventional steel or reinforced concrete MR frame structures. In detail, energy dissipation is concentrated both in column web panels which are not surrounded by concrete and in composite beam-to-column connections. A full-scale two-storey composite building was used to validate the system performance of composite MR frames with partial strength joints. The frame structure was subjected to pseudo-dynamic (PsD) tests at the European Laboratory for Structural Assessment (ELSA) of Joint Research Centre (JRC), in order to simulate the structural response under ground motions corresponding to earthquake hazards for a high-seismicity site with 10 % and 2 % chance of exceedence in 10 years. The ground motion for 10 % chance of exceedence in 10 years earthquake hazard caused minor damage while the one for 2 % chance of exceedence in 10 years earthquake hazard entailed column web panel yielding, connection yielding and plastic hinging at column base joints. An earthquake level chosen to approach the collapse limit state induced more damage and was accompanied by further column web panel yielding, connection yielding and inelastic phenomena at column base joints without local buckling. Successively, the structure was subjected to a final quasi-static cyclic test with interstorey drift ratios up to 4.6 %. Extensive cracks in the slabs and failure of extended end plates at weld toes were observed. Moreover, test offered additional opportunities to examine construction methods and validate the performance of simulation FE models. Exploiting inelastic static pushover and time-history analysis procedures, behaviour factors, design overstrength factors and the ductility demand of the structure was estimated. Finally, behaviour factors and overstrength factors were identified and compared to code-specified assumptions.

¹ Full Professor, Dept. of Mech. and Struct. Eng., Univ. of Trento, Italy. E-mail: oreste.bursi@ing.unitn.it

² Full Professor, Dept. of Struct. Eng., University of Pisa, Italy. E-mail: s.caramelli@ing.unipi.it

³ Assistant Professor, Dept. of Struct. Anal. and Design, University of Naples, Italy. E-mail: fabbroci@unina.it

⁴ Senior Researcher, Joint Research Centre, European Commission. Ispra. E-mail: artur.pinto@jrc.it

⁵ Assistant Professor, Dept. of Struct. Eng., University of Pisa, Italy. E-mail: walter@ing.unipi.it

⁶ Senior Researcher, Joint Research Centre, European Commission. Ispra. E-mail: fabio.taucer@jrc.it

⁷ Full Professor, Dept. CGM, Ecole Polytechnique of Montreal. E-mail: tremblay@struc.polymtl.ca

⁸ Full Professor, Dept. of Mech. and Struct. Eng., Univ. of Trento, Italy. E-mail: riccardo.zandonini@ing.unitn.it

INTRODUCTION

During the last two decades, a vast research effort has been promoted by the European Union to improve the knowledge in the domain of earthquake resistance of steel-concrete composite MR frame structures and their components. Composite structures exhibit indeed higher stiffness than steel structures and therefore, sway frames less sensitive to second-order effects can be realised. Such structures also show fire protection characteristics superior to those of steel structures. In slabs, composite systems eliminate the need for formwork.

Under the ICONS TMR European project [1], information on experimental studies was collected to form the basis of design provisions on reinforced concrete partially-encased columns [2]. The project also allowed typical details for bolted beam-to-column connections to be defined, though the design was addressed towards costly full strength beam-to-column joints. Since 1996, additional tests have been performed in Europe. This research effort was focussed on composite beams, and aimed at investigating the possible advantages provided by the stiffness and the plastic resistance of composite beams [3]. Therefore, several tests and analyses were carried out along this line [4-10]. This extensive experimental effort, combined with the evaluation of numerous experimental data and the development of some numerical models allowed design rules for composite MR frames with limited sway and full strength composite connections to be developed. Moreover, design guidelines were drafted and relevant rules are now included in the recently issued pr-EN version of the Eurocode 8 (EC8) [2]. Nonetheless, EC8 covers mainly traditional design options, and not in an exhaustive way. More specifically, dissipative zones could be advantageously located in partial strength beam-to-column connections and/or column web panels. This type of structural system is explicitly recognized in United States seismic design codes [11] and several tests have been performed in Europe and United States; see [12] and [13], among others. Moreover, relationships between ductility requirements in MR partially restrained frames and behaviour factor values stated in EC8 [2] have not been fully investigated.

These issues represent fundamental aspects of research and code developments on the seismic design of composite steel-concrete MR frame structures and are the issues that two European projects [14,15] are exploring through full-scale testing of substructures and 3D structures [16] as well as development of adequate models for partial strength composite joints in view of parametric analyses [17]. In detail, a full-scale two-storey composite building designed according to current seismic EC8 provisions with partial strength joints was subjected to pseudo-dynamic tests at the ELSA Laboratory of JRC in order to simulate the structural response under ground motions corresponding to earthquake hazards for a high-seismicity site with 10 % and 2 % chance of exceedence in 10 years. The corresponding maximum interstorey drift values exhibited by the structure were 0.71 % and 2.6 %, respectively. These ground motions induced different damage levels. Successively, the structure was subjected to an earthquake level able to induce the collapse limit state with an interstorey drift limit of 4.57 %; and to a final cyclic test inducing severe damage in beam-to-column joints, slabs and column base joints.

Tests offered additional opportunities to examine construction methods and validate the performance of simulation FE models. In fact, inelastic static pushover and time-history analyses allowed the behaviour factor, the design overstrength factor and the ductility capacity of the structure to be estimated. Finally, these tests also provided the starting point to explore vibration-based identification techniques in view of post-earthquake damage assessment [18] of structures designed with modern seismic design codes.

DESIGN OF TEST STRUCTURE

The seismic design of the 3D prototype structure illustrated in Fig. 1 is based on a MR concept for the longitudinal direction and a braced frame concept for the transversal one. European standards [2, 19-22] were followed. The 2-storey structure has dimensions 12 m x 12 m x 7 m and includes five two-bay MR frames with unequal spans of 5 m and 7 m, respectively. All five MR frames are identical and one of them

is illustrated in Fig. 2. In the transversal direction, the lateral resistance is provided by two concentrically braced steel frames located along the exterior walls. The structure tested at the ELSA Laboratory of JRC included only three MR frames as shown in Fig. 3. The total weight of the bottom and top storeys is 453.7 kN and 415.4 kN, respectively. Weights of 518.4 kN and 496.2 kN were added at the bottom and top storeys, respectively, to reproduce initial stresses in the slab. Masses relevant to bottom and top storeys employed in PsD tests were equal to 83269 kg and 85561 kg, respectively.

The interfloor distance is 3500 mm as indicated in Fig. 1. The beams of MR frames are IPE300 sections acting compositely with the 150 mm thick concrete slab. The slab was poured on a 55 mm deep trapezoidal composite steel deck Brollo with EGB210 profile and the slab flutes were spaced at 150 mm and oriented perpendicular to the main beam axis. $\phi 19$ mm shear studs were arranged in pairs to guarantee full shear connection. The composite slab extended on each side 700 mm in the transversal direction and 500 mm in the longitudinal one; this lay-out allowed proper development of the effective breadth and the slab anchoring for exterior beam-to-column joints. The columns shown in Fig. 4 are partially encased composite columns, which are deemed to guarantee significant structural efficiency with respect to static, seismic loads and fire resistance. They are connected at their bases with column base joints and continuous over the full height of the structure as drawn in Fig. 2. The steel profiles are HEB260 and HEB280 for the exterior and interior columns, respectively. Longitudinal $\phi 12$ mm and transversal $\phi 8$ mm rebars were located in concrete parts of columns and $\phi 19$ mm shear studs were used to ensure composite action between concrete and steel as well as to transfer shear from composite beams to columns. At the base and near beam-column joints, stirrups were spaced at 50 mm for both column types. Elsewhere, the spacing was increased to 150 mm. Column base joints were endowed with 40 mm thick extended end plates. They were connected to the foundation by means of 6 anchor bolts made with $\phi 32$ mm threaded hooked reinforcing bars. A 150 mm long stub part of a HEB140 profile was welded under each base plate to transfer horizontal shear to the foundation. Base plate stiffeners were installed on each column side to improve joint fixity.

Beam-to-column joints represent main dissipative elements of MR frames. Therefore, they were designed as innovative partial strength joints to provide adequate structural strength and ductility under cyclic loading. Therefore, subassembly tests were conducted prior to large-scale structure tests [17]. The design of beam-to-column joints sought limited strength degradation and plastic rotation capacity greater than the 35 mrad which are required by EC8 [2] to composite joints in MR frames of ductility class H. To this aim, a relatively thin 15 mm end-plate connection has been designed as illustrated in Fig. 4. It guarantees predictable and efficient performance for seismic actions. On the basis of constructional considerations as well as of favourable seismic behaviour of column web panels [9], the solution adopted relies on naked steel columns. In detail, the reinforced concrete encasement is interrupted in the connection and a pair of stiffening plates, set horizontally and welded to the column, guarantees full exploitation of the web panel's inelastic resources. Additional $\phi 12$ mm longitudinal and transversal rebars are placed in the floor slab close to joints. Transversal rebars can help develop concrete struts in order to transfer beam bending moments between beams and columns. Transverse beams are IPE240 sections and simple beam-to-column shear connections are used at their ends. No shear studs are welded to these beams and transverse lateral bracing, viz. X-bracing angles, are provided for lateral stability.

Nominal specifications for structural materials were: Class S235 ($f_y = 235$ MPa, $f_u = 360$ MPa, $f_u > 1.15 f_y$, $\epsilon_u > 15$ %) for structural steel; Class C25/30 ($f_{ck} = 25$ MPa) for concrete; and Class B450-C ($f_y = 450$ MPa, $f_u > 1.15 f_y$, $f_u/f_y < 1.35$, $\epsilon_u \geq 7.5$ %) for rebars. Measured material strength values of steel members, steel plates, concrete and reinforcing bars were higher than nominal values, especially for structural steel. EC8 on the other hand recommends that actual yield stress of steel be such as not to modify the location of plastic hinge regions assumed during design. In order to avoid storey mechanisms owing to extremely wide scatter of material strength values, the capacity design criterion of members and components of partial strength joints was performed [14-17]. As a result, measured material properties did not modify the location of yielding regions enforced through the capacity design criterion.

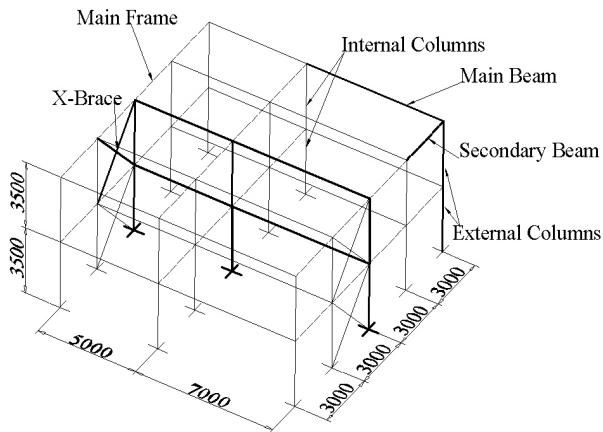


Fig. 1. 3D steel-concrete composite structure with partially encased columns (Dim. in mm)

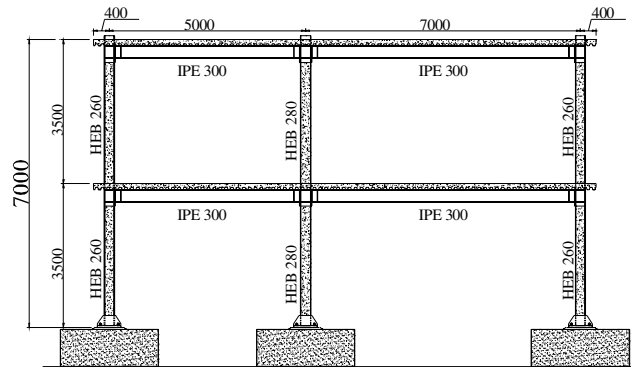


Fig. 2. Transversal view of a 3D test structure endowed with 3 MR frames

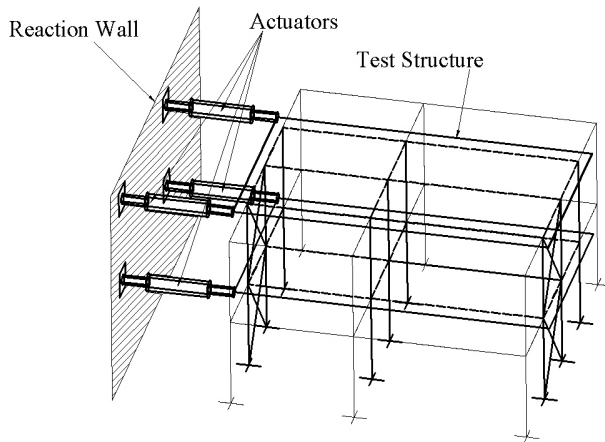


Fig. 3. 3D view of test structure

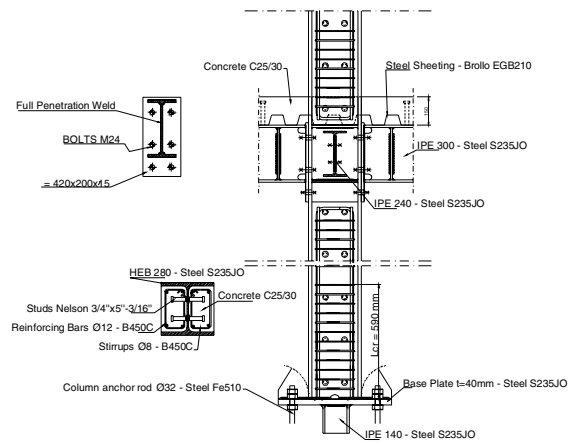


Fig. 4. View of: a partial strength joint; a partially encased column; a column base joint

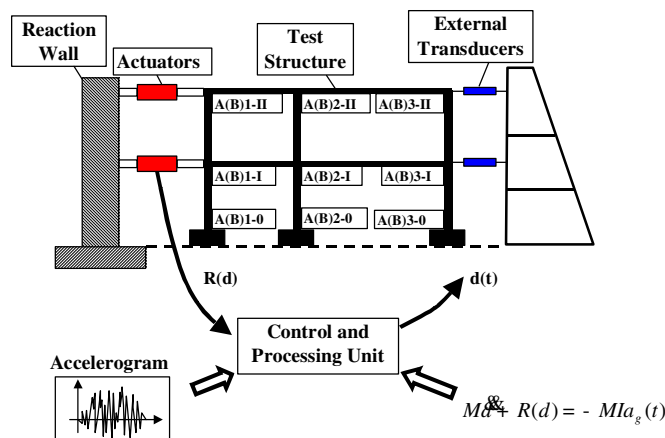


Fig. 5. Equipment and test structure for the pseudo-dynamic test method

EXPERIMENTAL PROGRAMME

Selection of earthquakes

In order to investigate the most probable lateral strength and inelastic demands imposed on the specimen, as well as to run PsD tests, suitable artificial accelerograms were selected. The accelerogram employed in the PsD technique is illustrated in Fig. 6. It is characterized by a strong motion duration of about 10 sec with rise and decay periods of 2.5 and 5.0 sec, respectively. It was sorted out from three artificial accelerograms, referred to A-03, A-12 and A-14, respectively, matching Type 1 elastic response spectrum of EC8 [2]. The spectrum derives from ground type A and 5 % viscous damping. The choice of artificial earthquakes is justified by the need of exciting the test structure with maximum forces at natural frequencies.

The generation of these accelerograms was done according to the procedure provided in [23]. At the end of the generation process, a linear baseline correction was applied to each record in order to remove residual drifts in displacement and velocity time histories. The single accelerogram employed for PsD tests was sorted out based on the highest level of damage induced in beam-to-column joints and limited value of damage induced in columns and base joints owing to the need of avoiding loss of stability at column bases. The resulting accelerogram A14 is illustrated in Fig. 6 together with the resulting elastic response spectrum shown in Fig. 7 and matching Type 1 spectrum. The efficacy of the baseline correction can be appreciated from the history of the ground displacement reported in Fig. 8.

In line with the Performance-Based Seismic Engineering philosophy, larger seismic demands were imposed through several pga levels employed in the PsD method as reported in Table 1. In detail:

1. an elastic PsD test in order to evaluate dynamic elastic properties of the structure, viz. eigenvalues, eigenvectors and equivalent viscous damping. Moreover, the accuracy both of the PsD algorithm and of set-up was checked;
2. a PsD test in order to simulate the structural response under ground motions corresponding to earthquake hazards for a high-seismicity site with 10 per cent chance of exceedence in 10 years. The earthquake should lead the structure to the elastic limit corresponding to the Serviceability Limit State of EC8 [2];
3. a PsD test in order to simulate the structural response under ground motions corresponding to earthquake hazards for a high-seismicity site with 2 per cent chance of exceedence in 10 years. The earthquake should lead the structure to the Ultimate Limit State corresponding to inelastic rotations in partial strength beam-to-column joints equal to about 35 mrad and degraded strength limited to 20 per cent. Some yielding is expected in column base joints;
4. a PSD test in order to bring the test structure at the Collapse Limit State;
5. a final cyclic test run according to the ECCS 45 procedure [24] with increasing amplitude cyclic displacements in order to induce a severe amount of damage in beam-to-column joints, column base joints and columns in a controlled and systematic way.

Testing techniques

In order to run both PsD tests and the final cyclic test two actuators and relevant external digital transducers were employed for each storey. The schematic of the PsD test exploited in this research is illustrated in Fig. 5. The digital controller, which treats numerical and experimental data of the test structure performs also the numerical integration of the overall system exploiting the Continuous PsD method with an explicit α -Newmark method and a time step size of 2 msec [25]. Inclometers and transducers were adopted in order to measure the rotation capacity of partial strength beam-to-column joints, as shown in Fig. 9. Moreover, strain gauges were used to monitor deformations in reinforcing bars close to beam-to-column joints and column flanges. Only an interior and an exterior frame of the test structure were instrumented with inclinometers, displacement transducers and strain gauges.

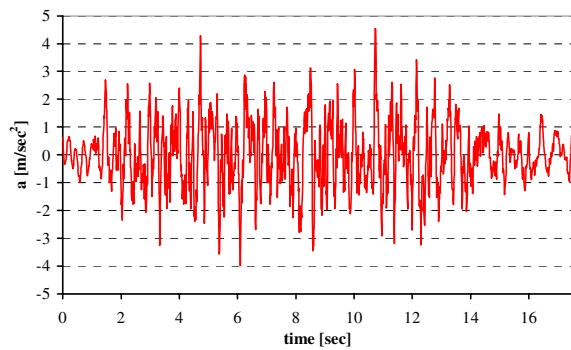


Fig. 6. Time history of artificial accelerogram A14 matching Type 1 EC8 spectrum

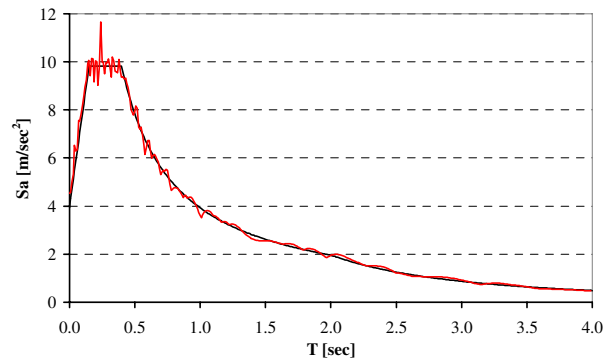


Fig. 7. Response spectrum of accelerogram A14 matching Type 1 EC8 spectrum

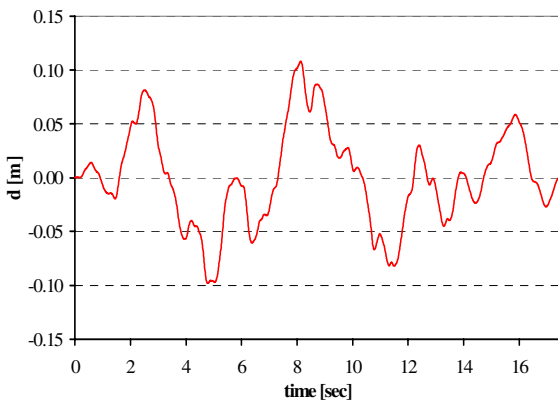


Fig. 8. Time history of ground displacement obtained from artificial accelerogram A14

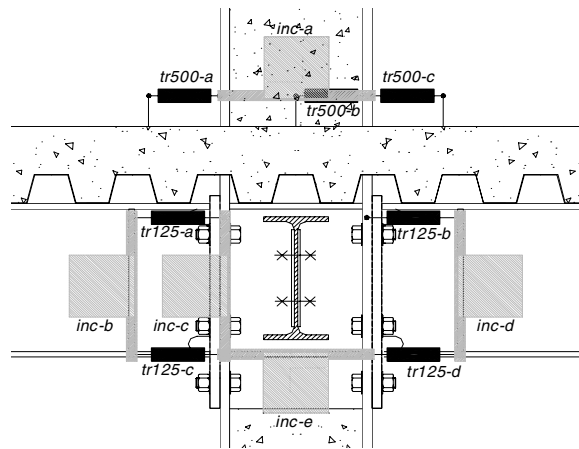


Fig. 9. Measurement equipment of partial strength beam-to-column interior joint

Table 1. Summary of pseudo-dynamic and cyclic tests

PsD Test N.	PGA [g]	Performance Objective
1	0.10	Elastic behaviour
2	0.25	Serviceability Limit State (No damage in structural parts)
3	1.40	Ultimate Limit State (joints' plastic rotation of about 35 mrad and strength degradation limited to 20 per cent)
4	1.80	Collapse Limit State
Cyclic Test	---	Maximum top displacement equal to 300 mm

MAIN EXPERIMENTAL RESULTS

Non-linear static and dynamic time-history analyses were performed using IDARC2D [26] prior to PsD tests. As a result, earthquakes with suitable accelerations were selected for each limit state sought. The rotational behaviour of beam-to-column joints and column base joints was simulated with hysteretic rotational springs located at the end of rigid or beam-column elements as illustrated in Fig. 10. Conversely, the web panel shear distortion was reproduced with a mechanical idealization which involves 4 rigid bars connected together by pins and rotational springs. Other modelling details of the mechanical model of column base joints are sketched in Fig. 11, while the entire FE of a 2D frame is depicted in Fig. 12. Columns and beams were introduced by using frame elements with spread plasticity. The behaviour of frame sections and rotational springs was simulated by means of a smooth hysteretic model developed by Sivaselvan and Reinhorn [27]. Hysteretic parameters of beam-to-column joints were calibrated on test results of subassemblages performed at the University of Pisa [16], while those of column sections were computed by fibre section analysis [14].

Results of the PsD test N. 2 with p_{ga} equal to 0.25 g

The objective of this test was to approach the onset of yielding with no excessive damage into the structure. The frame structure exhibited natural frequencies of 2.08 and 7.36 Hz for the flexural first and second mode, respectively. From a first visual inspection no damage occurred at columns bases; neither crushing nor spalling of concrete and nor local buckling in column steel flanges; thin cracks developed transversally in the mortar under base plates in line with hooked rebars; there was no visible gap between extended end plates and column flanges; cracks developed in the concrete slab.

Cracks induced into the slab were found to be more evident at the bottom storey and in external beam-to-column joints. Therefore, damage seemed to be more pronounced on exterior frames than the interior one, probably due to a larger effective breadth of the slab of second one, combined with possible in-plane deformations of the floor diaphragm at each storey. On the interior side of columns in beam-to-column joint areas cracks developed mainly parallel to transverse beams in line with or in front of interior columns; while on the exterior one, an inclined cracking pattern formed under hogging bending moment. From measurement equipment it was possible to evaluate rotations of beam-to-column joints. Maximum rotations reached by column web panels, connections and joints are shown in Fig. 13. Similar values were obtained for the interior frame. Note that positive rotations are clockwise. In detail, rotation values of web panels and connections correspond to maximum joint rotations. One may observe that rotations are larger at the bottom storey. The maximum rotation of base joints of internal frame was about -1.68 mrad. Experimental and predicted values of top storey displacement and base shear are illustrated in Fig. 14 and 15, respectively. The relevant agreement is satisfactory.

Results of the PsD test N. 3 with p_{ga} equal to 1.4 g

The frame structure exhibited natural frequencies of 1.94 and 7.01 Hz for the flexural first and second mode, respectively. From a visual inspection of beam-to-column joints, damage was located largely at the bottom storey close to the reaction wall and on exterior frames as understood from Fig. 16. Shear yielding of web panel at interior joints was observed, while at exterior joints a flexural yielding of end plates was noticed. However, only little permanent deformations could be observed in steel elements. The simulation provided by IDARC2D in terms of top storey displacement is illustrated in Fig. 17 and experiment and prediction data agree each others.

Cracks width increased in the slab and spalling of compressed concrete owing to excessive bearing against columns was observed at the bottom storey, as depicted in Fig. 18. This phenomenon appeared only at the interior side of beam-to-column joints. Gaps between steel column flanges and concrete slabs were also observed both at interior and exterior beam-to-column joints.

Neither damage nor cracking and nor local instabilities was observed at column bases. Nevertheless, rotations at column base joints was observed during the test. This was mainly due to an extension of

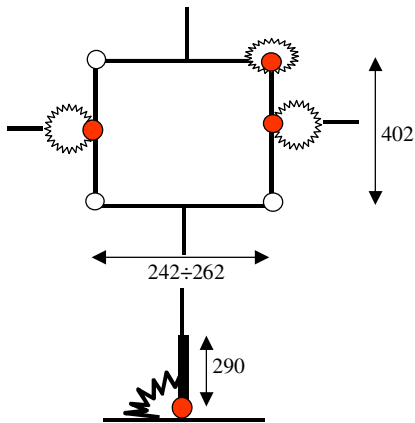


Fig. 10. FE model of an interior partial strength joint and column base joint

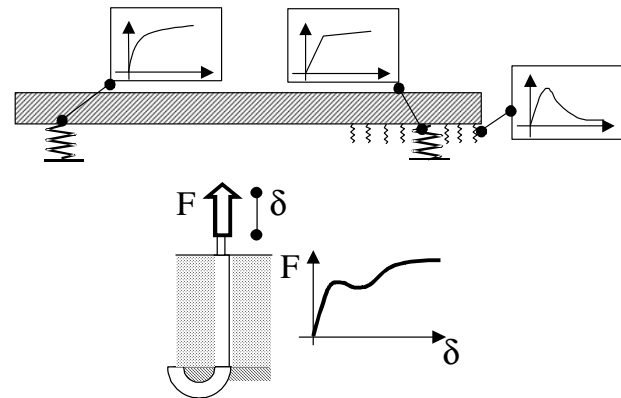


Fig. 11. Components of a mechanical model of a column base joint

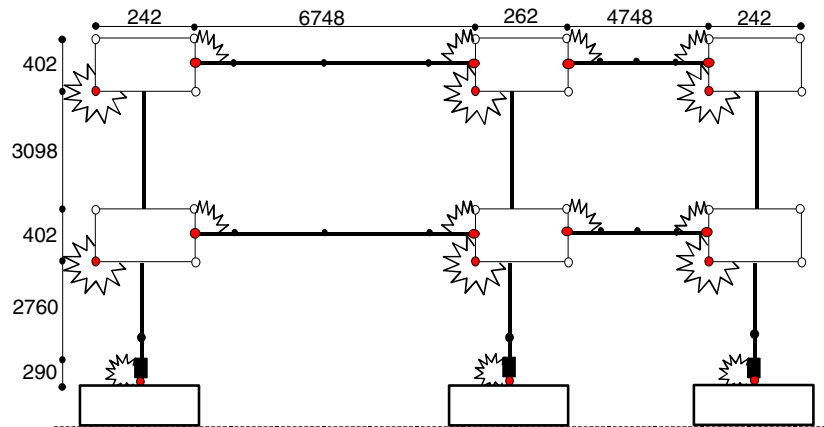


Fig. 12. 2D model of the test frame structure

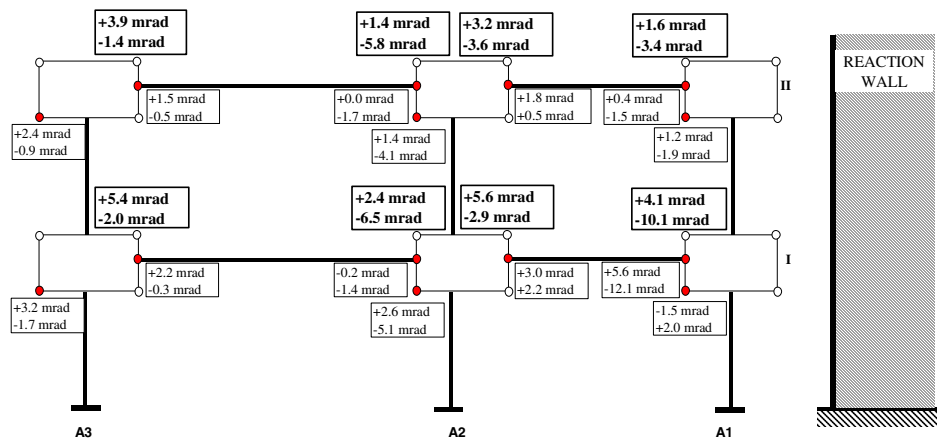


Fig. 13. Distribution of maximum values of rotations reached by column web panels, beam-to-column connections and joints of exterior frame during the PsD test N. 2 ($p_g = 0.25 g$)

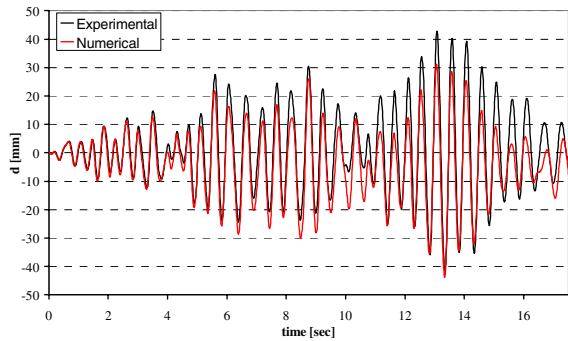


Fig. 14. Experimental and predicted displacement of the top storey at a pga = 0.25 g

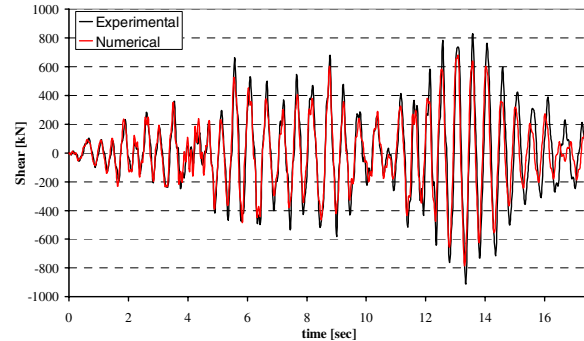


Fig. 15. Experimental and predicted base shear at a pga = 0.25 g

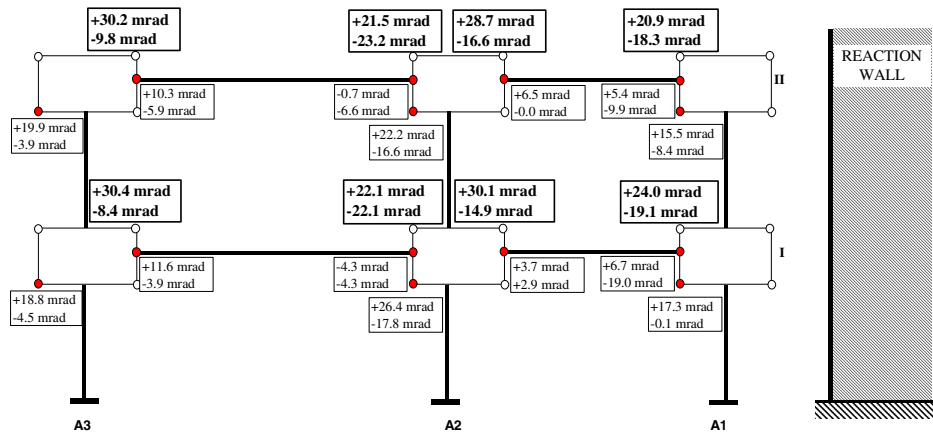


Fig. 16. Distribution of maximum values of rotations reached by column web panels, beam-to-column connections and joints of exterior frame during the PsD test N. 3 (pga = 1.4 g)

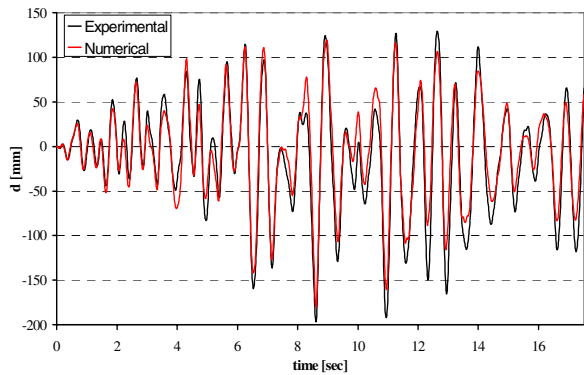


Fig. 17. Experimental and predicted displacement of the top storey at a pga = 1.4 g



Fig. 18. Failure in the concrete slab on an exterior joint of an exterior frame at a pga=1.4g

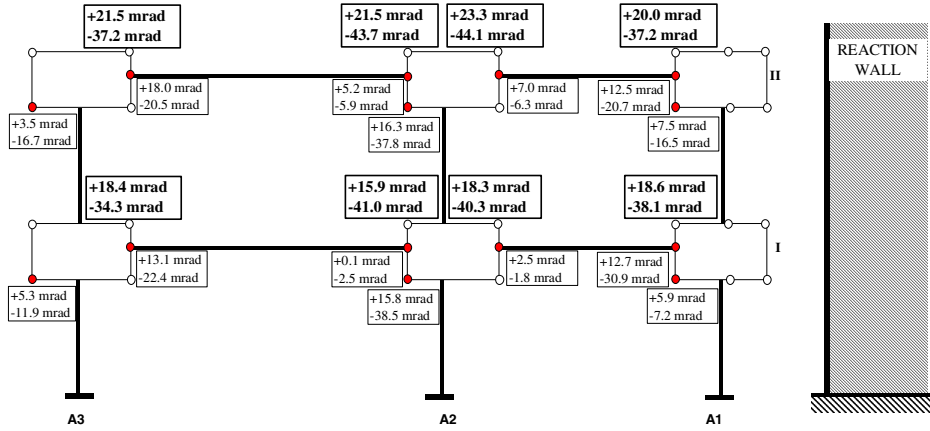


Fig. 19. Distribution of maximum values of rotations reached by column web panels, beam-to-column connections and joints of exterior frame during the PsD test N. 4 (p_{ga} = 1.8 g)

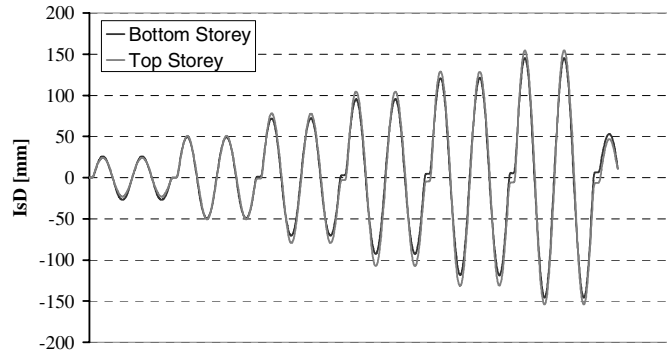


Fig. 20. Bottom and top storey interstorey drift measured during quasi-static cyclic test

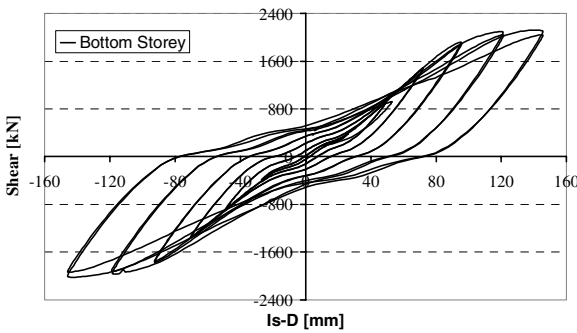


Fig. 21. Hysteretic loops of bottom interstorey drift-shear during quasi-static cyclic test

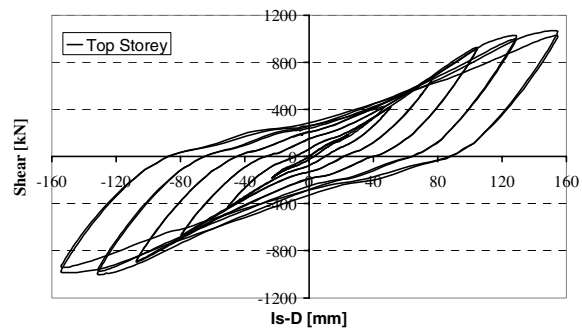


Fig. 22. Hysteretic loops of top interstorey drift-shear during quasi-static cyclic test

column anchor rods, and failure of the grout in compression. In detail, yielding of anchor rods occurred. The processing of experimental results entailed that no beam-to-column joint reached plastic rotations of 35 mrad. Moreover, maximum rotations of joints at the bottom and top storeys were quite similar while column web panels of the interior frame rotated more than the exterior frames. The maximum rotation of base joints of the interior frame was about -11.76 mrad.

Results of the PsD test N. 4 with pga equal to 1.8 g

The objective of this PsD test with an imposed pga equal to 1.8 g was to induce a Collapse Limit State on the test structure. The frame structure exhibited frequencies of about 1.17 and 5.46 Hz for the flexural first and second mode, respectively. From visual inspection and evaluation of experimental results both the behaviour of beam-to-column joints and column base joints was comparable to that of joints in the previous PsD test. Maximum rotation values of beam-to-column joints and components deformations increased as illustrated in Fig. 19. At column bases neither concrete cracking nor local buckling was observed. Yielding of anchorages in column base joints was evident. The maximum rotation of column base joints of the interior frame was about 24.14 mrad.

Results of the Final Cyclic test

The final cyclic test was performed by imposing interstorey drift ratios of about 4.6 % at the second storey, taking into account that the structure exhibited in the previous PsD test a residual displacement at the top storey of about 100 mm. The ratio of the reaction force at the bottom and at the top storey was fixed to 0.97. Such ratio was estimated by considering both modes derived from a modal analysis of the test structure after the PsD test N. 4. Imposed interstorey drifts are illustrated in Fig. 20 while the relevant hysteretic loops interstorey drift-storey shear relevant to the test structure are presented in Fig. 21 and 22 for the bottom and top storeys, respectively. An attentive reader can observe both a limited strength degradation and a limited stiffness deterioration of the structural response. The maximum interstorey drift of 4.6 % was reached at the 12th cycle. The instrumented exterior beam-to-column joint of the exterior frame close to the reaction wall exhibited cracks with a width similar to those observed after the PsD test N. 4; whereas exterior joints of exterior frames opposite to the reaction wall showed additional diagonal cracks starting from inner column flanges. From the processing of experimental data it was observed that beam-to-column joints rotated more at the bottom storey than at top one. Again, interior and exterior frames exhibited a similar behaviour. Moreover, the beam-to-column joint behaviour was quite similar under sagging and hogging moments. This phenomenon was probably caused by the severe cracking induced in the composite slab during previous PsD tests.

INELASTIC STATIC PUSHOVER AND DYNAMIC ANALYSIS PROCEDURES

Both the FE model illustrated in Fig. 12 and PsD results allowed behaviour factors and design overstrength factors to be estimated, respectively, by means of non-linear static pushover and dynamic analyses. Moreover, the reliability of inelastic static pushover analysis in predicting correctly the inelastic seismic demand was checked.

The non-linear static pushover analysis was performed using the Performance Point Method proposed in EC8 [2], employing the base shear force and the top storey displacement as force and displacement parameters. Two lateral force distributions were imposed on the FE model of Fig. 12: the first one characterized by a uniform shape and the second one by the first modal shape. Vertical loads were included in the analysis in order to induce both a reduction of initial stiffness and of natural frequencies of the structure. The Incremental Dynamic Analysis (IDA) was performed employing the trapezoidal rule in the implicit α -Newmark time-stepping scheme, with a single correction. Time steps were set equal to 0.001 and to 0.0001 sec for elastic and inelastic analyses, respectively.

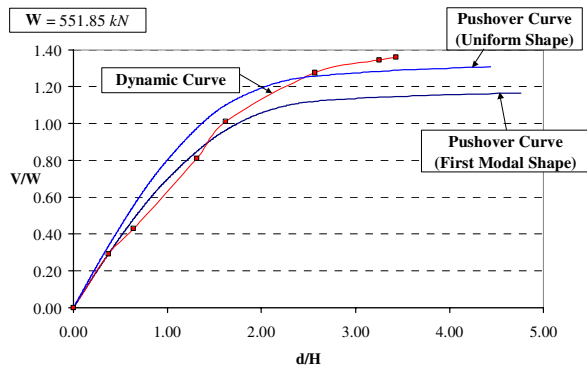


Fig. 23. First modal shape and uniform pushover analysis with dynamic analysis

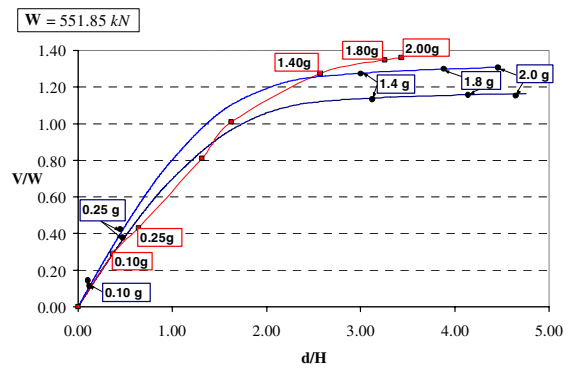


Fig. 24. Pga levels relevant to pushover and incremental dynamic analysis

Table 2. Results of non-linear static pushover and incremental dynamic analysis

Pga	Eurocode 8 pushover analysis				IDA	
	First Modal shape		Uniform shape		Displ.[mm]	Shear [kN]
	Displ.[mm]	Shear [kN]	Displ.[mm]	Shear [kN]		
0.10 g	16.22	108.98	15.69	115.75	23.41	164.16
0.25 g	40.57	265.38	39.24	283.45	43.70	253.08
1.40 g	227.19	638.04	219.76	717.10	179.88	720.22
1.80 g	292.10	649.34	282.60	734.03	227.84	759.60
2.00 g	324.60	654.98	313.94	739.68	240.08	768.22

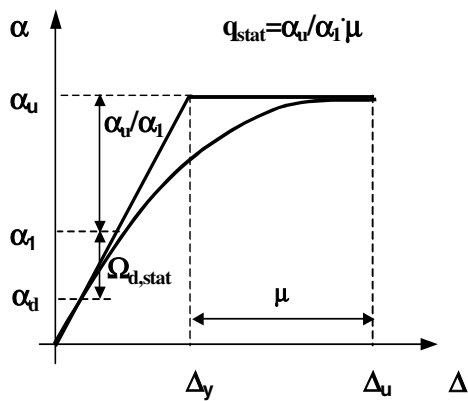


Fig. 25. Behaviour factor and overstrength factor relevant to static pushover analysis

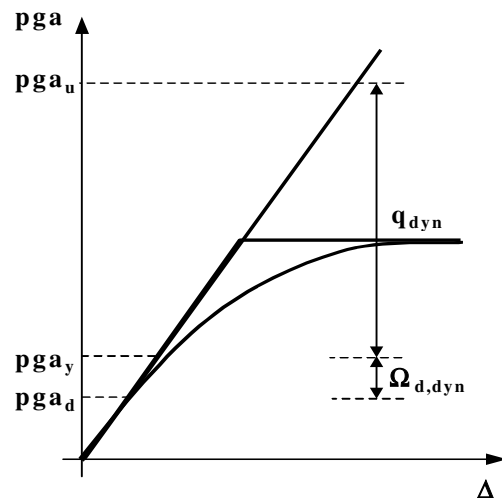


Fig. 26. Behaviour factor and overstrength factor relevant to incremental dynamic analysis

Response curves provided by FE analyses are plotted in Fig. 23 and 24, respectively, where $W = 551.85$ kN represents the design weight of each 2D frame. Pushover response curves provided by the uniform and first modal shape did not represent upper and lower limits of the dynamic response curve as evident for the elastic and early inelastic range. This trend is in line with observations highlighted in [28]. Moreover, the dynamic curve exceeded the uniform response curve for a pga at about 1.4 g.

Target performance points evaluated with static pushover analysis at five pga levels, see Fig. 24, are collected in Table 2 together with values provided by IDA analysis. One may observe maximum displacement errors of about 35 % between static pushover and dynamic analysis.

Numerical results allowed behaviour factors q_{stat} and q_{dyn} to be estimated. In detail, the behaviour factor q_{stat} was obtained from a non-linear static pushover curve by means of the following formula:

$$q_{stat} = \frac{a_u}{a_1} m, \text{ where } \alpha_u = 1.164 \text{ and } \alpha_1 = 0.459 \text{ define lateral load multipliers inducing on the structure}$$

the ultimate limit state and the elastic limit state, respectively; relevant base shears can be obtained by the design weight factor W ; $m = \frac{D_u}{D_y}$ is equal to 3.11, and represents the displacement ductility factor as

illustrated in Fig. 25. The behaviour factor q_{stat} reads 7.89.

Conversely, the behaviour factor q_{dyn} was tracked by means of the dynamic response curve through the formula: $q_{dyn} = \frac{pga_u}{pga_y}$, where $pga_u = 1.54$ g corresponds to a peak ground acceleration inducing a plastic

rotation in beam-to-column joints of about 35 mrad; $pga_y = 0.25$ g corresponds to the first yielding of the structure. A schematic representation of the behaviour factor q_{dyn} is illustrated in Fig. 26. The value of q_{dyn} reads 6.16 which is not far from the value $q_d = 6.0$ assumed in design [14,15].

The aforementioned analyses allow design overstrength factors $\Omega_{d,stat}$ and $\Omega_{d,dyn}$ indicated in Figs. 25 and 26, respectively, to be estimated. In particular, the following formulae were used: $W_{d,stat} = \frac{a_1}{a_d}$, where α_d

= 0.163 defines the lateral load multiplier at design level; and $W_{d,dyn} = \frac{pga_y}{pga_d}$, where

$$pga_d = \frac{a_g}{q_d} = \frac{0.40g}{6} = 0.067g \text{ defines the design peak ground acceleration. Therefore, } \Omega_{d,stat} \text{ and } \Omega_{d,dyn}$$

read 2.81 and 3.75, respectively. These overstrength values are not unusual in design and depend on the following factors: i) partial safety factors adopted during the design of the structure; ii) the design action amplification factor for accidental torsional effects; iii) enforced interstorey drift limits in order to satisfy the serviceability limit state; iv) design constraints provided by non-seismic actions; v) difference between nominal strength and measured strength of materials; vi) use of discrete standard dimensions of steel section profiles. It is worthwhile to mention that factors iii) iv) and v) were decisive factors for the design of this structure and hence for design overstrength values.

CONCLUSIONS AND PERSPECTIVES

The objective of this study has been the investigation of the seismic performance of a realistic size moment resisting frame structure of high ductility class according to Eurocode 8, under various levels of earthquake. Dissipative elements were conceived to be partial strength beam-to-column joints and column base joints at later stages. The construction of the full-scale structure proved that the construction of steel-concrete composite structures with partial strength beam-to-column joints and partially encased columns is highly efficient.

Pseudo-dynamic and cyclic test results confirmed that properly designed and constructed partial strength beam-to-column joints and partially encased columns without concrete in column web panels exhibit a favourable behaviour in terms of energy dissipation, limited strength degradation and ductility.

Analytical studies suggest that FE models of 2D frames assembled using IDARC2D were effective in capturing overall seismic response of the specimen especially when hysteretic elements are exploited to simulate components of beam-to-column joints and column base joints as well. Numerical analyses conducted by means of inelastic static pushover and time-history dynamic analysis procedures allowed behaviour factors and design overstrength factors to be estimated and compared to code-specified assumptions.

A detailed comprehension of internal actions of the structure in members and joints clearly imposes further study. Moreover, vibration-based identification techniques which were carried out in different stages of pseudo-dynamic tests in view of post-earthquake damage assessment require a detailed evaluation. Finally, simulation and implementation in FE codes of the deteriorating behaviour of dissipative components of beam-to-column and column base joints by means of robust hysteretic models deserve additional studies.

ACKNOWLEDGEMENTS

The results presented in this work were obtained in the framework of two European research projects, viz. the ECOLEADER HPR-CT-1999-00059 and the ECSC 7210-PR-250 project, for which the authors are grateful. However, opinions expressed in this paper are those of the writers and do not necessarily reflect those of the sponsors.

REFERENCES

1. ICONS Topic 4 Extended Group, A., "Draft of a section 6 to Eurocode 8, Part 1.3. Specific rules for steel concrete composite buildings", ICONS Project Report, University of Liege. 1998.
2. prEN 1998-1. "Eurocode 8: Design of structures for earthquake resistance. Part 1: General rules, seismic actions and rules for buildings", CEN, 2003.
3. Plumier, A. "European research and code developments on seismic design of composite steel concrete structures", Proc. of the 12th World Conf. on Earth. Eng., Auckland, Paper 1147, 2000.
4. Bouwkamp J, Parung H, Plumier A, "Bi-directional cyclic response study of a 3D composite frame." Proceedings of the 11th European Conference on Earthquake Engineering, Paris, 1998.
5. Doneux C, Parung H, "A study on composite beam-column subassemblages", Proceedings of the 11th European Conference on Earthquake Engineering, Paris, 1998.
6. Plumier A, Doneux C., "Dynamic tests on the ductility of composite steel-concrete beams", Proceedings of the 11th European Conference on Earthquake Engineering, Paris, 1998.
7. Manfredi G, Fabbrocino G, Cosenza E, "Modeling of steel-concrete composite beams under negative bending", Journal of Engineering Mechanics 1999; ASCE, 125(6): 654-662.
8. Bursi OS, and Gramola G, "Behaviour of composite substructures with full and partial shear connection under quasi-static cyclic and pseudo-dynamic displacements." Materials and Structures, 2000; RILEM, 33, 154-163.
9. Bursi OS, and Ferrario F, "Computational Models for the Low-cycle Fatigue Behaviour of Composite Members and Joints" in Progress in Civil and Structural Engineering Computing, Saxe-Coburg Publications, Stirling, 2003.
10. Thermou GE, Elnashai AS, Plumier A, Doneux C, "Seismic design and performance of composite frames", Journal of Constructional Steel Research 2004; 60: 31-57.
11. American Institute of Steel Construction, "Seismic provisions for structural steel buildings", AISC 341-02, AISC, Chicago, 2002.

12. Simoes R, Simoes da Silva L, "Cyclic behaviour of end plate beam-to-column composite joints.", *Steel and Composite Structures* 2001; 1(3): 355-376.
13. Green PT, Leon RT, Rassati GA, "Bidirectional tests on partially restrained, composite beam-to-column connections", *Journal of Structural Engineering* 2004; ASCE, 130(2): 320-327.
14. Bursi OS, Caramelli S, Fabbrocino G, Molina J, Salvatore W, Taucer F, "3-D Full-scale Seismic Testing of a Steel-concrete Composite Building at Elsa", Contr. No: HPR-CT-1999-00059, Eur Report, European Community, 2004.
15. Caramelli S, Salvatore W. et al., "Applicability of Composite Structure to Sway Frames, ECSC Project n. 7210-PR-250, Eur Report, European Community, 2004.
16. Braconi A, Bursi OS, Ferrario F, Salvatore W, "Seismic design of beam-to-column connections for steel-concrete composite moment resisting frames.", *Proceedings of the 4th Int. Conf. STESSA 2003: Behaviour of Steel Structures in Seismic Areas*. Naples, Italy, 2003, 253-260.
17. Salvatore W, Braconi A, Bursi OS, Tremblay R, "Modelling of a partial-strength beam-to-column joint for high ductile steel-concrete composite MR frames" *Proceedings of the 13th World Conference on Earthquake Engineering*, Vancouver, Canada, Paper no. 2929. 2004.
18. Bursi OS, Molinari M, Nardini L, Salvatore W, Zonta D, "Vibration-based identification and assessment of a 3D composite MR frame structure at different damage levels" *Proceedings of the 13th World Conference on Earthquake Engineering*, Vancouver, Canada, Paper no. 2812. 2004.
19. prEN 1991-1-1. "Eurocode 1: Actions on structures, Part 1-1: General actions, densities, self-weight, imposed loads for buildings", CEN, 2003.
20. prEN 1992-1. "Eurocode 2: Design of concrete. Part 1: General rules and rules for buildings", CEN, 2003.
21. prEN 1993-1. "Eurocode 3: Design of steel structures. Part 1: General rules for buildings", CEN, 2003.
22. prEN 1994-1, "Eurocode 4: Design of composite steel and concrete structures. Part 1: General rules for buildings". CEN, 2003.
23. Clough RW, Penzien J, "Dynamics of Structures" Second Edition, McGraw-Hill, 1993.
24. Technical Committee 13, "Recommended testing procedures for assessing the behaviour of structural steel elements under cyclic loads." ECCS no. 45, 1986.
25. Magonette G, Pegon P, Buchet P, Bonelli A, "Continuous pseudo-dynamic testing with non-linear substructuring", *Proceedings of the 2nd European Conf. on Struc. Control*, Paris, July, 2000.
26. Valles RE, Reinhorn AM, Kunnath SK, Li C, Madan A, "IDARC2D Version 4.0: A Program for the Inelastic Damage Analysis of Buildings", Technical Report NCEER-96-0010, 1-8, 1996.
27. Sivaselvan MV, Reinhorn AM, "Hysteretic Model for Cyclic Behaviour of Deteriorating Inelastic Structures", Technical Report MCEER-99-0018, 1999.
28. Antoniou S, Rovithakis A, Pinho R, "Development and verification of a fully adaptive pushover procedure", *Proceedings of the 12th European Conf. on Earth. Engin.*, London, Paper no. 822, 2002.